Electrochemically fabricated ultrafine metal masks for the fabrication of two-dimensional materials-based devices

Running title: Electrochemically fabricated ultrafine metal masks for the fabrication of two-dimensional materials-based devices

Running Authors: Jianwen Zhong et al

Jianwen Zhong[1], Zhao Sun[1], Han Li[1], Zhuofei Gan[1], Chuying Sun[1], Yi Wan[1], Lain-Jong Li[1], and Wen-Di Li[1,a)]

[1]Department of Mechanical Engineering, University of Hong Kong, Hong Kong, China

[a)] Electronic mail: liwd@hku.hk

Transition metal dichalcogenides (TMDs) are considered promising candidates for the next generation of electronic building blocks in integrated circuits due to their superior performance in mitigating various challenges such as short channel effects. Optical photolithography and electron beam lithography are commonly employed for fabricating electrical contacts and patterning TMDs to create electronic devices. The atomic layer structure of TMDs is highly susceptible to external conditions, making conventional lithography methods, which often leave undesirable polymer residues and involve high-energy electron radiation, not ideal for achieving high devices performance. Shadow mask lithography, a method free of polymers and radiation, has been used to define electrodes and etch patterns on these sensitive materials, avoiding the need for photoresists and electron irradiation. Nevertheless, there remains a significant gap in efficiently producing reusable and flexible masks, particularly with high-resolution feature sizes, for defining metal electrodes on patterned or curved substrates for practical applications. Additionally, the use of metal masks for etching or defining patterns on

these emerging atomic thin layer materials is underutilized. In this study, we introduce a novel, cost-effective electrochemical method for manufacturing reusable and flexible metal masks with ultrafine feature sizes. By combining electroplating techniques with the dry transfer method, we have successfully produced metal masks with ultrafine features, which were then utilized to evaporate metal electrodes with submicron feature sizes onto nanostructured substrates. These metal masks, with specifically designed patterns, were employed as etching masks to pattern monolayer MoS_2 (a type of TMD) materials without the need for photoresists or solution processes. Moreover, the resulting metal mask-evaporated electrodes, with smooth edges, were integrated with atomic layer transition metal dichalcogenides through van der Waals (vdW) interactions to create devices based on MoS_2. The successful fabrication of MoS_2-based devices on patterned substrates has enabled us to investigate the effect of strain engineering on modulating the performance of these devices.

I. INTRODUCTION

Two-dimensional materials (2D materials) are increasingly investigated and explored as promising candidates for the next generation of electronic and optoelectronic devices, given their superior electronic, optical, and mechanical properties compared to their bulk counterparts[1-3]. The family of 2D materials encompasses various elements and combinations, including graphene[4], hexagonal boron nitride (hBN)[5], black phosphorus (BP)[6], and transition metal dichalcogenides (TMDs)[7]. Among these materials, TMDs have garnered significant attention as next-generation semiconductors, poised to meet the demands of scaling down transistor sizes in the post-silicon era. TMDs exhibit rich layer-

dependent electron band diagrams and naturally ultra-thin thicknesses of just one or a few atomic layers. However, due to their extremely thin atomic layer structures, TMDs are highly susceptible to the manufacturing process, particularly when it comes to establishing electrical contacts between metal electrodes and the TMDs. Conventional techniques for fabricating metal electrodes, such as optical lithography (OL) or electron beam lithography (EBL), pose challenges for monolayer TMDs, leaving behind photoresist residues and subjecting the material to high electron radiation. For example, when EBL is used to define electron resist patterns with high electron energy, the channel materials of TMDs may become doped or even damaged, resulting in the creation of defects within the channels. Residual photoresists randomly distribute on the contact region and increase contact resistance of devices, so large variation exists among different devices even in a same fabricated patch[8]. Furthermore, polymer residues present limitations in enhancing the performance of TMD-based devices. Additionally, conventional lithography techniques involving spincoating, developing, and lift-off may introduce unexpected dopants to TMDs and are not suitable for solution-vulnerable 2D materials[9].

Another critical step is the patterning of channel materials to construct TMD-based devices. Recently, large-scale monolayer films of TMDs with fewer crystal boundaries have been directly synthesized on specific substrates using chemical vapor deposition (CVD) with various precursors[10,11]. Although large films of TMDs pave a bright future for electronic devices and integrated circuits, there remains a gap in realizing TMD-based devices across a wide range of applications. This is because the transfer and patterning processes on the target substrate in the post-processing stage

inevitably introduce contaminants, defects, and cracks. Various methods have been adopted to pattern TMDs into designed arrays, including photolithography[12,13], plasma-assisted nano-printing[14], selectively peeling off[15], scratching lithography[16], and direct laser writing[17]. Among these methods, optical lithography is commonly used to fabricate a photoresist mask layer for etching excess areas of TMD films. During the etching process, inductively coupled plasma etching (ICP-RIE) or reactive ion etching (RIE) are typically employed to etch TMD materials, leading to degraded photoresists due to plasma bombardment and implantation, making it challenging to remove residual photoresists. Moreover, some organic solutions used in lithography processes can degrade plastic substrates commonly used for fabricating flexible and wearable devices with TMD materials. Transfer printing can result in non-uniform layers and patterns of materials and involves complex lithography-based fabrication steps for obtaining printed stamps of materials[14]. Although resist-free laser writing is a facile method using commercial techniques, its scalability is limited due to the time-consuming nature of the serial process and the high cost of femtosecond lasers[17]. To overcome above constraints, there is a pressing need to develop innovative lithography technologies for fabricating TMD-based devices and circuits without introducing contamination, doping, or damage to the atomic layer materials.

The development of lithographic methods suitable for TMD layer materials has garnered significant attention from both laboratory research and industry, aiming to enhance the performance of devices. Stencil lithography (SL) stands out as a solvent-free and non-irradiated technique for patterning metal electrodes and functional materials, utilizing designed mask apertures to guide the flow of atoms, ions, molecules, or particles

for deposition or etching[18,19]. With its solvent-free process and material compatibility advantages, stencil lithography emerges as an ideal method for manufacturing TMD-based devices and exploring novel materials. This technology offers a promising alternative to traditional fabrication methods and enables the investigation of new material possibilities. To broaden the application scope of mask lithography, enhancing resolution and enabling pattern processes on curved or patterned surfaces are crucial goals. From a geometrical view, improving the resolution of shadow mask methods involves minimizing the blurring and shadowing effects. The blurring effect can be reduced by narrowing the gap between masks and target substrates, while the shadowing effect can be mitigated by thinning the shadow mask thickness[20,21]. Early efforts focused on enhancing pattern resolution by utilizing rigid SiN_x masks[22,23]. Other types of rigid silicon masks have been employed to fabricate 2D material devices to boost device performance[24-28]. Although Si mask have significantly improved performance of graphene and MoS_2 transistors, the rigidity of these masks results in a gap between the mask and target substrates, limiting conformal contact. Moreover, Si and SiN_x masks are costly and require complex fabrication processes involving vacuum deposition, electron beam lithography, and ion etching, further restricting their scalability to small applications.

In order to address limitations, researchers have proposed the use of ultrathin and soft polymer masks as a viable solution to reduce blurring and shadowing effects by ensuring conformal contact between masks and substrates. Soft polymethyl methacrylate (PMMA) has been employed to create shadow masks for defining patterned structures and fabricating 2D material devices[29-32]. However, due to the fragility of PMMA thin

films, manipulating the PMMA mask poses a challenge, as it can easily break when applied to pattern structures on target regions. Additionally, the organic polymer molecules in the PMMA film make it susceptible to certain chemical materials and high-temperature processes, resulting in lower reusability compared to rigid Si and SiN_x masks. Although the performance of MoS_2-based devices fabricated using PMMA masks has improved, the fabrication process involving electron beam lithography and specific transfer procedures leads to low productivity and mask reusability[33]. Similarly, ultrathin polyethylene terephthalate (PET) film has been utilized to create high-performance devices as shadow masks. The manufacturing process of PET masks involves using thin thermal release tape as a support, gold conductive film deposition, and focused ion beam etching, making this mask costly with low reusability[34]. Therefore, there is a need to explore an inexpensive approach to develop a shadow mask with high reusability and mechanical flexibility to enhance stencil lithography applications.

In our research, we have introduced an innovative method for manufacturing highly reusable and flexible metal masks to advance stencil lithography applications. Nickel metal masks with customized patterns have been successfully produced using non-vacuum electroplating techniques. Nickel metal exhibits high chemical and mechanical resistance, making it a durable and reusable mask for establishing contact with and detaching from target substrates during deposition or etching procedures. Moreover, the entire metal mask can be easily and completely detached from the plating substrate to become a stand-alone mask. With few micrometers thickness of electrodeposited nickel mask, it allows to conformally deposit metal electrodes on curved or patterned surface. Furthermore, metal masks have been utilized to pattern MoS_2

channel arrays on both flat and nanostructured substrates using reactive ion etching methods. To showcase the smooth edge of the deposited metal electrode achieved with this nickel metal mask, MoS_2 flakes have been van der Waals (vdW) integrated with pre-fabricated electrodes to construct MoS_2-based devices. Additionally, we have explored strain engineering through imprinting within MoS_2 devices, which has led to a significant enhancement in photocurrent and optical responsivity in MoS_2-based photodetectors. This type of metal mask introduces a new approach for patterning and fabricating TMDs materials, opening up possibilities for working with other solvent-sensitive materials as well.

II. EXPERIMENTAL PROCEDURE

A. Fabrication process of ultrafine nickel metal masks

First, commercial indium tin oxide (ITO) glass substrates were cleaned by sequentially immersing them in acetone, isopropanol (IPA), and deionized (DI) water for ultrasonication for 10 minutes each. Subsequently, the ITO glass was dried using a flow of nitrogen gas and then placed in an oxygen plasma cleaner chamber for surface cleaning for 2 minutes. Next, AZ 1518 photoresist was spincoated onto the ITO glass to achieve a film of 2.8μm thickness, with spincoating parameters set at 2000 rpm for 60 seconds. The spincoated sample was then pre-baked on a hot plate at 100°C for 90 seconds. Following this, the sample was exposed to UV light using a URE-2000/35 UV mask aligner (Chinese Academy of Sciences, China) with an exposure dose of 150mJ/cm^2. Subsequently, the sample was immersed in AZ 726 MIF developer for 60 seconds to develop the photoresist patterns. The sample was then rinsed in DI water and dried using a flow of nitrogen gas, as illustrated in Fig. 1(a). Secondly, a commercial

nickel-plating solution (Caswell, USA) was utilized as the electrodeposition solution. The Keithley 2400 source meter was employed to supply a constant current (e.g., 15 mA) to the two electrodes of the electroplating setup. The patterned photoresist on the ITO glass sample served as the working electrode, while a piece of nickel plate acted as the counter electrode. The thickness of the deposited nickel film on the ITO surface was regulated by adjusting the electroplating time, with the nickel mask thickness set at 3μm in this study. Following the electrodeposition process, the sample was immersed in DI water to thoroughly rinse off any residual solution and then dried using a flow of nitrogen gas, as depicted in Fig. 1(b). Subsequently, the sample was placed in acetone for 5 minutes to dissolve the photoresist, followed by rinsing in DI water. After removing the photoresist, the nickel metal mask remained on the ITO glass substrate, as illustrated in Fig. 1(c). The free-standing metal mask was obtained by peeling off the nickel film from the ITO glass, as demonstrated in Fig. 1(d), marking the completion of the metal mask fabrication process.

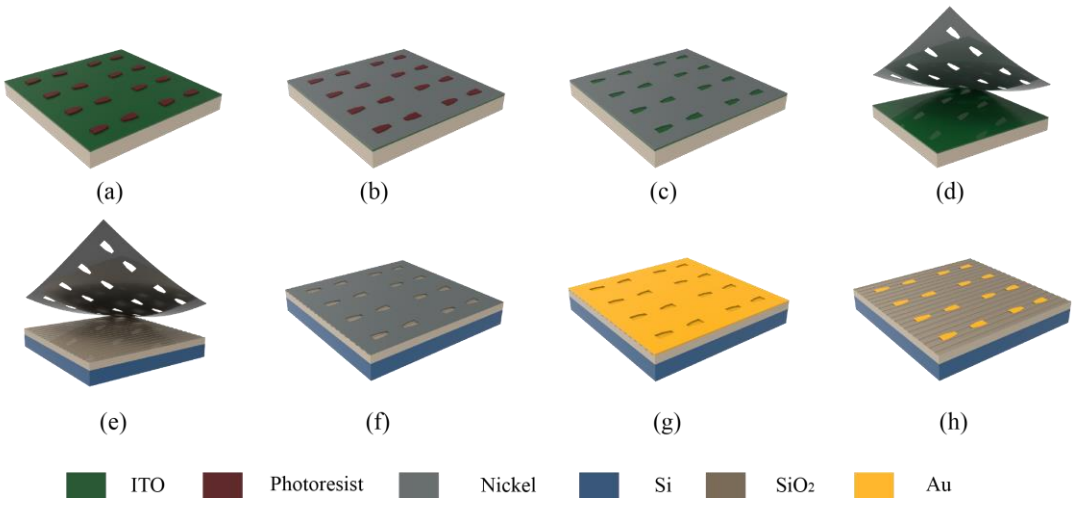

FIG. 1. Fabricated process of nickel metal mask and deposited metal electrodes on grating substrate. (a) Patterned photoresist on top of ITO glass. (b) Electroplated nickel metal

mask followed pre-defined photoresist patterns. (c) Dissolved photoresist after finishing electrodeposition. (d) Peeled off metal mask from ITO glass. (e) Contacted metal mask on top of grating substrate. (f) Metal mask completely laminated on target substrate. (g) Deposited gold electrodes followed apertures of metal mask. (h) Gold electrodes on top of grating substrate after peeling off metal mask.

B. Fabrication process of metal electrodes by the reusable ultrafine metal mask

The metal mask with micron-scale features was used to fabricate the metal electrodes for MoS_2 devices on a nanostructured substrate that introduced a patterned strain field through a nanoimprint-induced strain engineering process[35]. The nanostructured substrates containing grating patterns were fabricated by integrating an interference lithography patterning using a commercial patterning system (HIL-1000, InterLitho Technology Limited, Hong Kong SAR) with an inductively coupled reactive ion etching process. Initially, a SiO_2/Si wafer with grating patterns was aligned with the metal mask from one edge to the other. Once the metal mask covered the designated area, small magnets were employed to secure the metal mask in place on the sample. Subsequently, the samples affixed to the chuck were inserted into the thermal evaporator chamber holder. Gold electrodes, with a thickness of 60 nm, were evaporated under a pressure below $4*10^{-4}$ Pa, and the evaporation rate was maintained at approximately 0.1 nm/s. Prior to evaporating the gold electrodes, a thin layer of chrome was evaporated at 5 nm to enhance the adhesion between the gold electrodes and the grating substrates. Upon completion of the evaporation process, depicted in Fig. 1(g), the metal masks were gently

peeled off from the evaporated substrates using tweezers from a corner. Finally, clean and smooth-edged metal electrodes were obtained on the top of the grating substrates.

C. Etching MoS_2 using the ultrafine metal mask

The initial step involved transferring a monolayer of MoS_2 grown via chemical vapor deposition (CVD) from the sapphire substrate to the SiO_2/Si wafer, which featured a surface divided into half flat and half grating regions, using a PMMA-assisted method. Subsequently, the etching mask was aligned with the target substrate and secured in place using small magnets. Following this, reactive ion etching with oxygen plasma was employed to etch the uncovered areas of the MoS_2 material. The plasma etching power was maintained at 100 W for a duration of 20 s. Upon completion of the initial etching process, the MoS_2 material was defined, as illustrated in Fig. 2(b), with the pre-designed patterns on the metal mask. Building upon the initial etching step, a second type of metal mask was applied to the target area with optical alignment of the etching square area outline. In the final step, the MoS_2 material was etched following the aperture of the metal mask under the same plasma conditions. Subsequently, rectangular arrays of MoS_2 were obtained after removing the metal mask.

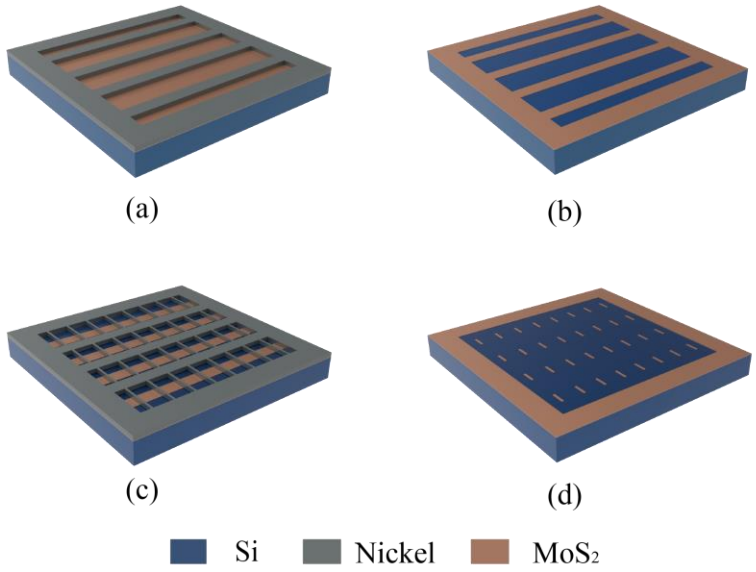

FIG. 2. Etching process of monolayer MoS_2 by using reusable metal mask. (a) Defined metal mask attached on top of MoS_2. (b) Peeling off metal mask after first etching process. (c) Secondly defined metal mask attached to first etched MoS_2 (d) MoS_2 patterned arrays after second etching process.

D. Transfer process of monolayer MoS_2 on top of metal electrodes

MoS_2 based devices were constructed by transferring MoS_2 flakes on top of metal electrode arrays using a PMMA assisted transfer process. The first step was to spincoat 3%-wt PMMA solution on top of MoS_2 substrate at 2000 rpm for 60 s. The PMMA layer was then baked at 100°C for 120 s and spincoated three times to achieve a PMMA layer thickness exceeding 1μm, ensuring good support during the transfer process. Second, the sample was immersed in a NaOH solution to separate the MoS_2, which is encapsulated in the PMMA layer, from the grown substrates. Then the PMMA layer was captured using a PDMS transparent layer, and water inside the sample was dried. MoS_2 flakes were

optically aligned to the pre-defined metal electrodes using a 2D materials transfer platform. By thermally releasing the PMMA layer from the PDMS layer at 90°C for 10 minutes, the MoS_2 flakes were transferred onto the fabricated metal electrodes. Finally, the PMMA layer was dissolved or selectively etched to enable performance measurements of the MoS_2-based devices.

E. Characterizations

Morphological characterization of samples was done with an optical microscope, a scanning electron microscope (SEM, Zeiss Sigma 300), and an atomic force microscope (AFM, Bruker MultiMode-8). The performance of the photodetectors was evaluated using a microscopic optoelectronic characterization system in an ambient chamber at room temperature. This system allowed for the precise measurement of various device parameters, such as electrical characteristics and optical response, to assess the functionality and performance of the photodetectors under specific conditions.

III. RESULTS AND DISCUSSION

A. Fabricated nickel metal mask

To demonstrate the fabrication process of metal masks, scanning electron microscopy (SEM) images of samples were characterized as shown in Fig. 3.

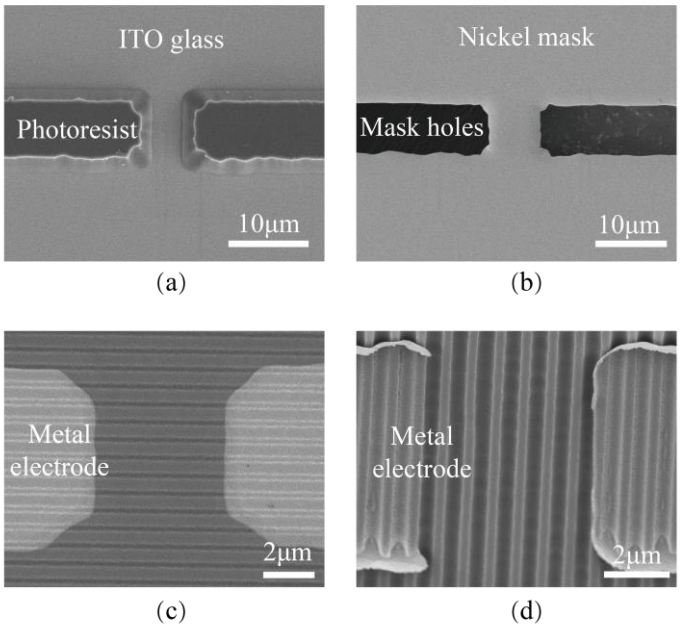

FIG. 3. (a) Patterned photoresist on ITO glass for electrodeposition. (b) Free-standing nickel metal mask after peeling off from ITO glass. (c) Metal electrodes fabricated by reusable metal mask on grating substrate. (d) Metal electrodes fabricated by conventional photolithography and lift-off process.

In Fig. 3(a), the image illustrates the developed photoresist (PR) pattern on the surface of ITO glass, clearly showing a channel gap between one pair of electrodes. Fig. 3(b) displays the feature size of a few micrometers on the free-standing nickel mask, with the black area representing the aperture area used for defining metal electrodes on the target substrate during the physical vapor deposition step. The micrometer-level thickness of the nickel metal mask allowed it to conformally attach to curved surfaces. Fig. 3(c) demonstrates the patterning of defined metal electrodes using the nickel mask after thermal evaporation. The metal electrodes were also conformal with the nanostructured substrate with surface relieve gratings, forming a continuous metal film on the grating substrate. The smooth edge of the metal electrode is highlighted as an important feature

for constructing MoS_2-based devices on top of these metal electrodes. Contrastingly, Fig. 3(d) shows metal electrodes fabricated using conventional photolithography techniques, displaying a warping edge that could be detrimental for integrating atomically-thin van der Waals (vdWs) materials.

B. Depositing metal electrodes on curved or patterned surfaces

Fig. 4(a) displays an optical image of a free-standing nickel mask with centimeter-scale sizes, featuring opening areas of 10x10 predefined electrode arrays for depositing metal electrodes onto various substrates through stencil evaporation. Fig. 4(b), (c), and (d) show the metal mask was applied to make contact with different substrates, including a flat Si wafer substrate, the curved surface of a solvent bottle, and a grating-patterned SiO_2/Si wafer. Following metal evaporation through this metal mask, it was possible to obtain 100 pairs of electrodes on a 10x10 mm^2 area with a featured channel gap of less than 5μm.

Fig. 4(e) and (f) demonstrate the feature sizes of two pairs of metal electrodes on grating substrates. Both sets of metal electrodes exhibit smooth edges without any warping and have clean surfaces without residual polymer due to the stencil deposition process. These characteristics are advantageous for constructing devices based on 2D materials.

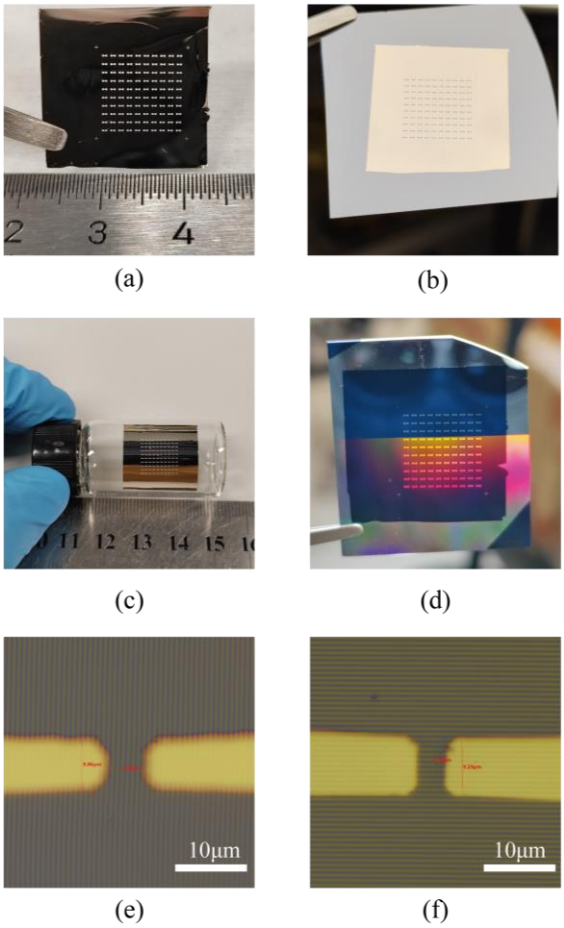

FIG. 4. (a) Free-standing nickel mask with a centimeter-scale size. (b) Metal mask contacted with Si wafer substrate. (c) Flexible metal mask attached on a curved surface of a solvent bottle conformally. (d) Metal electrodes fabricated by using the metal mask on patterned grating substrate. (e) and (f) Zoom in view of metal electrodes on patterned grating substrates.

C. Defining MoS_2 pattern arrays through etching using the metal mask

In the process of fabricating devices based on TMDs, defining TMD films into functional patterns is crucial. Fig. 5(a) and (b) depict an optical image of a fabricated nickel stencil mask used for dry-etching monolayer MoS_2 on a target substrate without

the need for any chemical treatment steps. This approach significantly reduces the risk of chemical contaminations that can occur during the fabrication process, especially for solvent-sensitive materials.

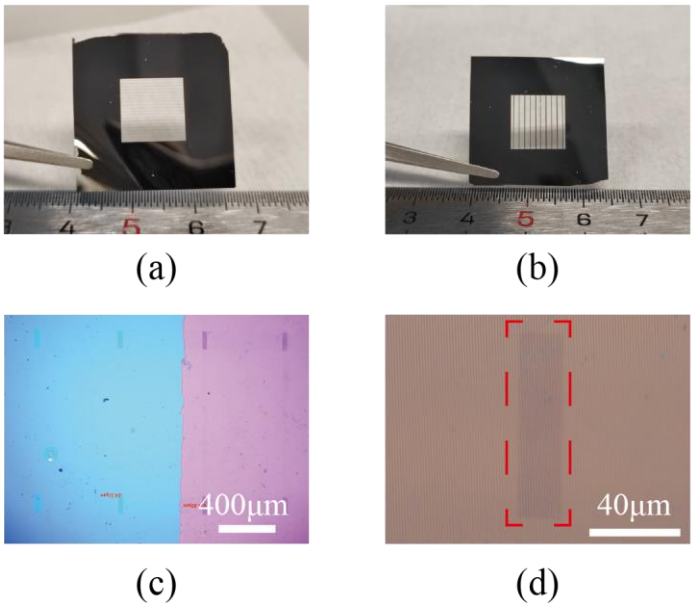

FIG. 5. (a) Free-standing nickel mask 1 with 25 μm wide stripes on a centimeter-scale size. (b) Free-standing nickel mask 2 with 100 μm wide stripes. (c) Patterned MoS_2 arrays on the grating and flat regions on the substrate. (d) Magnified view of one piece of patterned MoS_2 on the grating substrate.

Fig. 5(c) shows rectangular MoS_2 pattern arrays on a grating-patterned substrate without introducing photoresist contaminations, achieved by using the two metal masks as etching masks in two consequent etching processes. Fig. 5(d) presents a magnified view of the rectangular MoS_2 pattern from Fig. 5(c) on a grating substrate area with dimensions of approximately 25μm width and 100μm length. Following the shadow mask etching process, pre-fabricated metal electrodes could be transferred on top of the

patterned MoS_2 arrays using the van der Waals integration method. This method provides an effective way to investigate the intrinsic performance of MoS_2-based devices.

D. MoS_2 photodetectors with microscale electrodes fabricated using the ultrafine metal mask

We demonstrated the application of our ultrafine metal masks in the fabrication of MoS2 photodetectors with designed strain modulation. Here, the electrodes of the MoS2 photodetectors were deposited using the ultrafine metal mask through a stencil lithography process. Then, to facilitate the vdWs integration of MoS_2 flakes with pre-defined metal electrodes, a wet transfer process was employed. Illustrated in Fig. 6, a single MoS_2 flake was meticulously aligned optically onto the channel area between two electrodes. The figure depicts a flawlessly transferred MoS_2 flake, devoid of any cracks, conformally positioned atop the electrodes. The smooth edges of the metal electrodes play a crucial role in preventing the inadvertent penetration of the atomic layer MoS_2 flake during the integration process and the subsequent nanoimprint-induced strain engineering step, which is essential for inducing local strain in the MoS_2 flake.

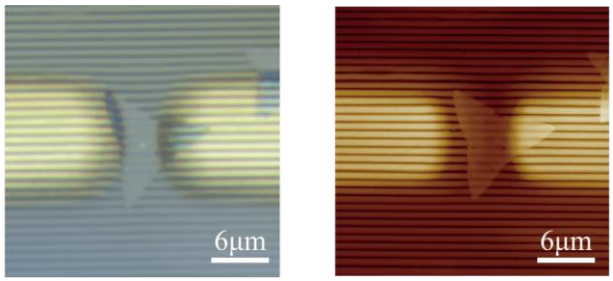

FIG. 6. (a) Optical image of a vdWs integrated MoS_2 photodetector after transferring materials on top of pre-defined metal electrode. (b) AFM image of a vdWs integrated MoS_2 photodetector after transferring materials on top of pre-defined metal electrode.

The pristine surface of the metal electrodes, fabricated using metal masks, ensured a clean electrical interface between the MoS_2 flake and the metal electrodes, as depicted in Fig. 6(b), showcasing the MoS_2 flake conformally adhering to the grating surface of the metal electrodes. This interface functioned as an ohmic resistive contact between the MoS_2 flakes and the electrodes, a characteristic validated by the linear trend observed in the output I-V curve of the devices in Fig. 7(a) and (b). The linear nature of the I-V curve indicated an ohmic constant resistance rather than a nonlinear Schottky barrier connection.

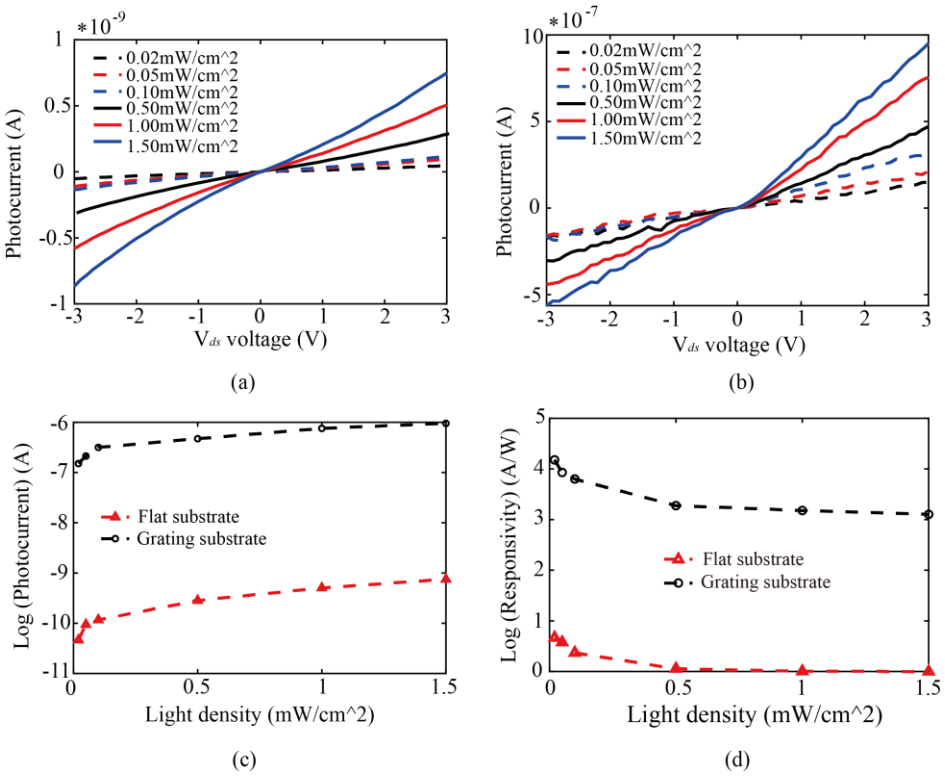

FIG. 7. (a) Photocurrent of MoS_2 on flat substrate without strain introduction. (b) Photocurrent of MoS_2 on grating substrate with introduced local strain by imprinting technique. (c) Logarithmic photocurrent of devices with strain on grating substrate and without strain on flat substrate. (d) Logarithmic responsivity of devices with strain on grating substrate and without strain on flat substrate.

Furthermore, the study delved into exploring the performance modulation of MoS_2-based devices. As illustrated in Fig. 7(c), devices incorporating strain engineering exhibited an enhancement of nearly three orders of magnitude in output current under varying light intensities compared to devices without strain engineering. As a result, the responsivity of the devices saw a significant improvement upon introducing local strain into the MoS_2 flake, as demonstrated in Fig. 7(d).

IV. SUMMARY AND CONCLUSIONS

This study showcases a novel method developed for producing reusable and flexible ultrafine metal masks through electrodeposition of nickel film on a patterned conductive substrate and mechanical separation. Utilizing this metal mask in stencil lithography evaporation, we have successfully defined micrometer-scale metal patterns on various substrates and surfaces. Additionally, we have employed the metal mask as an etching mask to pattern monolayer MoS_2 into rectangular arrays, avoiding the use of chemical solutions and preventing contamination. Subsequently, the creation of clean and smooth metal electrodes fabricated using these metal masks enabled the integration of MoS_2 flakes with pre-defined metal electrodes through a wet transfer process, and the fabricated MoS_2 photodetectors were used to investigate the effect of local strains in the photocurrent and photoresponsivity through nanoimprint-induced strain engineering. This strain engineering approach proved to be an effective method for enhancing the performance of MoS_2-based devices, resulting in a remarkable three-order-of-magnitude improvement in output current and responsivity. The metal masks introduced in this work are reusable and flexible with ultrafine patterns at the micrometer scale, and are

promising for being applied for fabricating solvent-sensitive TMD-based devices that need clean interfaces.

ACKNOWLEDGMENTS

This work was partially supported by the Research Grants Council of the Hong Kong Special Administrative Region (Awards No.17209320, C7018-20G, and AoE/P-701/20).

DATA AVAILABILITY

The data that support the finding of this study are available from the corresponding author upon reasonable request.

REFERENCES

[1]Liu, Y., Duan, X., Shin, H. J., Park, S., Huang, Y., and X. Duan, Nature, **7848**, 43(2021).

[2]Sheng, C., Dong, X., Zhu, Y., Wang, X., Chen, X., Xia, Y., and Bao, W, Advanced Functional Materials, **50**, 2304778(2023).

[3]Liu, C., Chen, H., Wang, S., Liu, Q., Jiang, Y. G., Zhang, D. W., and Zhou, P, Nature Nanotechnology, **7**, 545(2020).

[4]F. Schwierz, Proceedings of the IEEE, **101**, 1567(2013).

[5]Roy, S., Zhang, X., Puthirath, A. B., Meiyazhagan, A., Bhattacharyya, S., Rahman, M. M., and Ajayan, P. M. Advanced Materials, **33**, 2101589(2021).

[6]Xia, F., Wang, H., Hwang, J. C., Neto, A. C., & Yang, L. Nature Reviews Physics, **5**, 306(2019).

[7]Manzeli, S., Ovchinnikov, D., Pasquier, D., Yazyev, O. V., and Kis, A., Nature Reviews Materials, **8**, 1(2017).

[8]Shi, W., Kahn, S., Jiang, L., Wang, S. Y., Tsai, H. Z., Wong, D., and Zettl, A. Nature Electronics, **3**, 99(2020).

[9]Li, W., Tao, Q., Li, Z., Yang, G., Lu, Z., Chen, Y., and He, J. Nature Electronics, **7**, 131(2024).

[10]Yu, H., Huang, L., Zhou, L., Peng, Y., Li, X., Yin, P., and Zhang, G. Advanced Materials, **33**, 2402855(2024).

[11] Li, T., Guo, W., Ma, L., Li, W., Yu, Z., Han, Z., and Wang, X. Nature Nanotechnology, **16**, 1201(2021).

[12]Li, L., Peng, Y., Tian, J., Wu, F., Guo, X., Li, N., and Zhang, G. Nano Research, **16**, 12794(2023).

[13]Huang, B., Wang, Y., Li, L., Wang, Q., Peng, Y., Li, X., and Zhang, G. Nano Letters, **23**, 9333(2023).

[14]Nam, H., Wi, S., Rokni, H., Chen, M., Priessnitz, G., Lu, W., and Liang, X. ACS nano, **7**, 5870(2013)

[15]Zhao, J., Yu, H., Chen, W., Yang, R., Zhu, J., Liao, M., and Zhang, G. ACS Applied Materials & Interfaces, **8**, 16546(2016).

[16]Wei, Z., Liao, M., Guo, Y., Tang, J., Cai, Y., Chen, H., and Zhang, G. 2D Materials, **7**, 045028(2020).

[17]Poddar, P. K., Zhong, Y., Mannix, A. J., Mujid, F., Yu, J., Liang, C., and Park, J. Nano Letters, **22**, 726(2022).

[18]Vazquez-Mena, O., Gross, L., Xie, S., Villanueva, L. G., and Brugger, J, **132**, 236(2015).

[19]Du, K., Ding, J., Liu, Y., Wathuthanthri, I., and Choi, C. H. Micromachines, **8**, 131(2017)

[20]Sun, Y. C., Boero, G., and Brugger, J, **8**, 2201119(2023)

[21]Vazquez-Mena, O., Villanueva, L. G., Savu, V., Sidler, K., Langlet, P., and Brugger, J, Nanotechnology, **20**, 415303(2009).

[22]Deshmukh, M. M., Ralph, D. C., Thomas, M., and Silcox, J, Applied Physics Letters, **75**, 1631(1999).

[23]Vazquez-Mena, O., Sannomiya, T., Tosun, M., Villanueva, L. G., Savu, V., Voros, J., and Brugger, J, ACS nano, **6**, 5474(2012).

[24]Bao, W., Liu, G., Zhao, Z., Zhang, H., Yan, D., Deshpande, A., and Lau, C. N, Nano Research, **3**, 98(2010).

[25]Bao, W., Cai, X., Kim, D., Sridhara, K., and Fuhrer, M. S, Applied Physics Letters, **102**, 1831(2013).

[26]Song, X., Zan, W., Xu, H., Ding, S., Zhou, P., Bao, W., and Zhang, D. W, 2D Materials, **4**, 025051(2017).

[27]Zan, W., Zhang, Q., Xu, H., Liao, F., Guo, Z., Deng, J., and Zhang, D. W, Nano Research, **11**, 3739(2018).

[28]Zhang, H., Guo, X., Niu, W., Xu, H., Wu, Q., Liao, F., and Bao, W, 2D Materials, **7**, 025019(2020).

[29]Shih, F. Y., Chen, S. Y., Liu, C. H., Ho, P. H., Wu, T. S., Chen, C. W., and Wang, W. H, AIP Advances, **6**, 1978(2014).

[30]Yun, H., Kim, S., Kim, H., Lee, J., McAllister, K., Kim, J., and Wook Lee, S, Scientific reports, **5**, 10220(2015).

[31]Cai, H., Meng, Q., Ding, H., Zhang, K., Lin, Y., Ren, W., and Wang, X, ACS nano, **9**, 9626(2018).

[32]Cai, H., Meng, Q., Chen, Q., Ding, H., Dai, Y., Li, S., and Wang, X, Advanced Materials, **32**, 2002570(2020)

[33]Song, W., Kong, L., Tao, Q., Liu, Q., Yang, X., Li, J., and Liu, Y, Small, **17**, 2101209(2021).

[34]Han, B., Liu, B., Wang, G., Qiu, Q., Wang, Z., Xi, Y., and Hsu, H. Y, Advanced Functional Materials, **33**, 2300570(2023).

[35]Sun, C., Zhong, J., Gan, Z., Chen, L., Liang, C., Feng, H., and Li, W. D, Microsystems & Nanoengineering, **10**, 49(2024).